

THREE-LEVEL IMPROVED FULL-BRIDGE DC-DC CONVERTER FOR WIND ENERGY CONVERSION SYSTEMS

S.Madhananand¹, Dr.S.Senthilkumar²

¹PG Scholar, ²Assistant Professor

Department of Electrical Engineering, Government College of Engineering, Salem.

¹sivamadhan13@gmail.com

²Sengce2009@yahoo.in

ABSTRACT

The global demand for electric energy has continuously increased over the last few decades. As far renewable energy is concerned wind energy production plays a major role. A DC-DC converter is needed to connect the wind turbines to a DC grid. In general, three level full-bridge converter (TLFB) is employed for this purpose. This paper proposes a three level improved full-bridge (TLIFB) DC-DC converter for a wind turbine in a DC grid by inserting a passive filter into the DC-DC converter to improve the performance of the converter. The passive filter can effectively reduce the voltage stress of the medium frequency transformer (MFT) in the TLIFB DC-DC converter. This is very significant in the medium-voltage and high-power applications.

Keywords-DC-DC converter; dc grid; three-level full-bridge (TLFB).

I. INTRODUCTION

The dc grid, with the advantages such as reactive power, harmonics [2], seems to be a promising solution of power collection system for growing demand in the offshore wind power development. The offshore wind turbines may be directly connected into a dc grid to deliver dc power to a medium- or high-dc voltage network [6]. To realize the dc power delivery and connection, a high-efficient DC-DC converter is required. Normally, the voltage level of the dc network would be dozens of kilovolts which is too higher than the input voltage of the dc-dc converter [6]. Hence, a medium frequency transformer (MFT) operated at hundreds of hertz to several kilohertz could be installed in the DC-DC converter, which not only ensures that the input voltage can be boosted to a desired output voltage, but also achieves the galvanic isolation between the source and grid.

While considering the series parallel resonant converter, the peak current is high and the number of modules in the input switches is increased compared with the FB converter. Also, the voltage-stiff output limits the demanded voltage rating for the output bridge compared with the FB converter [10]. Besides, owing to the high-voltage level in the dc network, the usage of the diode bridges in the DC-DC converters could be advantageous.

A number of converters are presented in [12]–[17]. Among various configurations the two level and three-level configurations are mainly considered here, since both of the two configurations have been widely used in the wind energy conversion systems [1]. Fig. 1

shows several possible DC-DC converters for wind turbines in a DC grid, including the basic full-bridge (FB) two-level converter, the basic half-bridge(HF) three-level converter, the basic FB three-level converter, and the FB three-level converter based on submodules (SMs). Although the required number of switches for the FB two-level converter are not so many among the four configurations, the switches in the two-level configurations will take the full dc-bus voltage. The rate of change of voltage dv/dt is high; therefore, it may cause electromagnetic interference (EMI) [4], [12], [13]. As the three-level converters with the advantages in the aspects of power quality, semiconductor electrical and thermal stresses, and EMI for high-power applications [7], [8], [14], [15] the switches in the basic HB three-level converter, FB three-level converter, and the SMs-based FB three-level converter only take half of the dc bus voltage, which effectively reduces dv/dt in comparison with the FB two-level converter.

For the N-level configuration, a total number of $8(N-1)$ switches are needed for the SMs-based FB converter, which is much more than $2(N-1)$ and $4(N-1)$ switches required in the basic HB and FB converters, respectively [16], [17]. Besides, the corresponding numbers of voltage sensors are normally required for the SMs, and the voltage balancing control would be complicated for the SMs-based Full Bridge converter [11].

The basic three-level full-bridge (TLFB) converter, with the advantages of the reduced voltage stress of the switches, reduced filter size, and improved dynamic

response, is becoming highly suitable for medium-voltage and high-power conversion applications[17]. Although both the basic TLFB and the SMs-based TLFB configurations can create five-level output voltage to minimize voltage steps and reduce dv/dt in comparison with the HBTL configuration, particularly in the medium-voltage and high-power applications [3], [16], [18], the basic TLFB converter has simpler circuit structure and less number of switching devices than the SMs-based TLFB configuration, which leads

to a high reliability and small footprint for the basic TLFB converter.

In this paper, an improved TLFB (TLIFB) dc-dc converter is presented for an offshore wind turbine connected to a dc grid as shown in Fig. 2, where the TLIFB converter is applied to boost the dc input voltage from a diode rectifier to a high voltage for the dc grid integration.

This paper is organized as follows. In Section II, the TLIFB

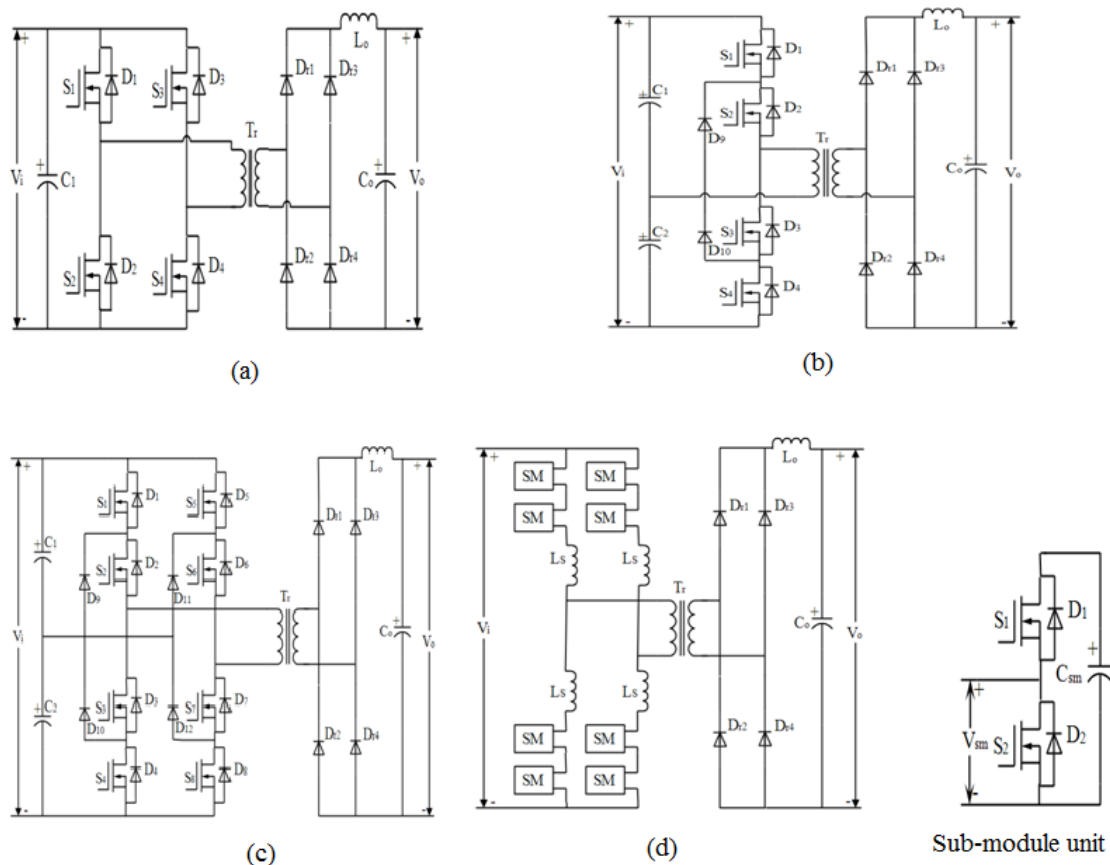


Fig. 1 (a) Basic FB two-level converter. (b) Basic three-level HB converter. (c) Basic three-level FB converter. (d) SMs based three-level FB converter.

TABLE I COMPARISON OF DIFFERENT CONVERTER TOPOLOGIES

Converter topology		No. of switches required	Valve voltage	Produced voltage level	Voltage balance control complexity	Voltage sensor
2 level	Basic FB converter	4	DC bus voltage	2	No	1
3 level	Basic HB converter	4		3	Easy	2
3 level	Basic FB converter	8		5	Easy	2
3 level	FB converter based on SMs	16	Half DC bus voltage	5	Calculation is proportional to the SMs number	8

DC-DC converter and the corresponding modulation strategy are proposed. The simulation results are given in Section III. The control circuit is made with 8051 microcontroller, IR2110 and tested. The description about the hardware setup of the control circuit of the proposed Three Level Improved Full Bridge (TLIMP) DC-DC converter is given in Section IV. The conclusions are drawn in Section V.

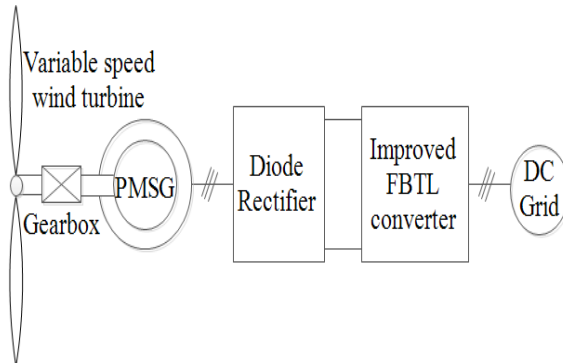


Fig. 2 Block diagram of the wind turbine connected to a dc grid.

and two capacitors (C_{i1} and C_{i2}). The capacitors C_{i1} and C_{i2} are voltage divided capacitors, which are used to split the dc bus voltage V_i into two equal voltages V_{c1} and V_{c2} . Different from the TLFB dc-dc converter, a passive filter is inserted into the TLIFB dc-dc converter as shown in Fig. 3 to improve the performance of the converter [9], which can effectively overcome the problem that the nonlinear characteristics of semiconductor devices results in distorted waveforms associated with harmonics and reduces the voltage stress of the MFT, which is very significant for the power converter in the high-power application.

B. Converter Operation

The switches S_1 – S_8 are switched complementarily in pairs with a pulse width modulation (PWM), i.e., pairs S_1 – S_3 , S_4 – S_2 , S_5 – S_7 , and S_8 – S_6 , respectively. D is the duty cycle for S_1 . The way of phase shifting the PWM for other switch pairs results in the different operation modes as follows.

1) *Operation Mode I*: The PWM waveform for the pairs S_8 – S_6 , S_5 – S_7 , and S_4 – S_2 lags behind the PWM waveform for pair S_1 – S_3 by $(D - D_c)T_s/2$, $T_s/2$, and $(D - D_c + 1)T_s/2$ respectively as shown in Fig. 4(a). T_s is the switching cycle. The overlap time

II. TLIFB DC-DC CONVERTER

A. Converter Description

Fig. 3 shows the circuit configuration of the TLIFB dc-dc converter, which is having eight switches (S_1 – S_8), eight freewheeling diodes (D_1 – D_8), four clamping diodes (D_9 – D_{12}), an MFT, four rectifier diodes (D_{r1} – D_{r4}), a passive filter (L_s and C_s), an output filter inductor L_d , an output capacitor C_o between S_1 – S_3 and S_8 – S_6 is $D_c T_s/2$, which is also for S_4 – S_2 and S_5 – S_7 . D_c is the overlap duty ratio.

2) *Operation Mode II*: The PWM waveform for pair S_8 – S_6 leads that for the pair S_1 – S_3 by $(D - D_c)T_s/2$, and the PWM waveform for the pairs S_4 – S_2 and S_5 – S_7 lags behind that for the pair S_1 – S_3 by $(1 - D + D_c)T_s/2$ and $T_s/2$, respectively, as shown in Fig. 4(b). $D_c T_s/2$ is the overlap time between both the pairs i.e. between S_1 – S_3 and S_8 – S_6 and between S_4 – S_2 and S_5 – S_7 .

The main difference between the two operation modes is the capacitor charge and discharge situations in each half cycle. In operation mode I, capacitor C_{i2} discharges more energy than capacitor C_{i1} in each half cycle as shown in Fig. 4(a), while capacitors C_{i1} and the C_{i2} exchange their situations in operation mode II as shown in Fig. 4(b). In operation mode II, capacitor C_{i1} discharges more energy than capacitor C_{i2} in each half cycle. The two operation modes can be alternatively used for the adaptive voltage balancing control.

In Fig. 4, voltages V_{ab} , V_{t1} , V_{t2} and currents i_{Ls} , i_{t1} , i_{t2} are all periodic waveforms with period T_s . Currents i_{c1} , i_{c2} , and i_L are with the period $T_s/2$. Owing to the passive filter in the TLIFB DC/DC converter, the performance of voltages V_{t1} , V_{t2} and currents i_{t1} , i_{t2} associated with the MFT is effectively improved, which is significant for the TLIFB DC/DC converter in the applications of the medium-voltage and high-power system. From Fig. 4, it is easy to see that the charge and discharge situations (i_{c1} and i_{c2}) of capacitors C_{i1} and C_{i2} are the main difference between the operation modes I and II, which would affect the capacitor voltages V_{c1} and V_{c2} . The other performances of the converter are nearly the same.

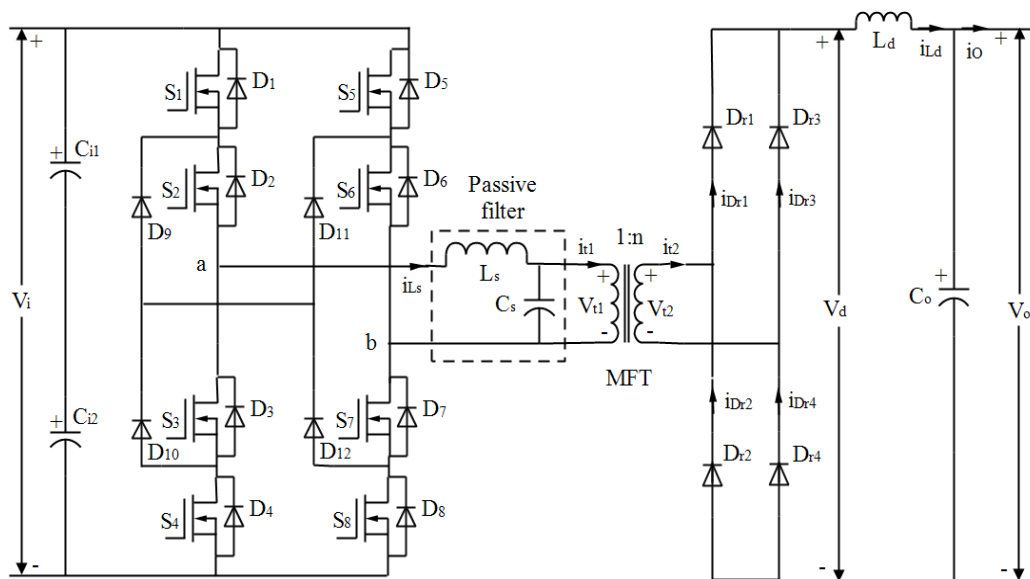


Fig. 3 Block diagram of the proposed TLIFB dc-dc converter.

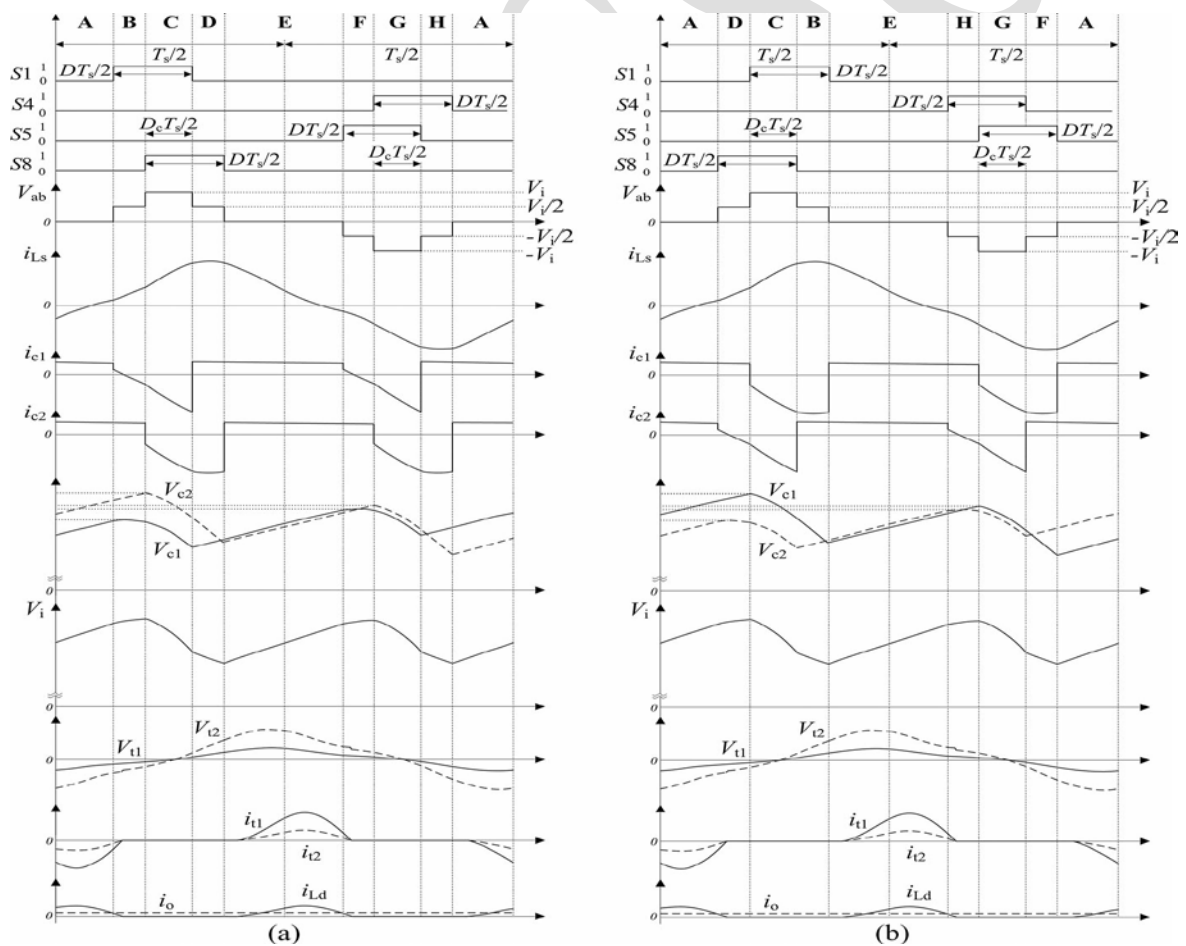


Fig. 4 Key waveforms of the TLIFB dc-dc converter. (a) In operation mode I. (b) In operation mode II.

TABLE III Simulation parameters

Parameters	Value
Input voltage, V_i	100 V
Output voltage, V_o	300 V
Input capacitors, C_{i1} and C_{i2}	3300 mF
Filter inductance, L_s	1.4 mH
Filter capacitor, C_s	300 μ F
Transformer turns ratio, N	2.6
Inductance, L_d	100 mH
Capacitor, C_o	1000 μ F
DC network resistance	100 Ω

III. SIMULATION RESULTS

To verify the theoretical analysis of the proposed topology, the simulation results are presented using PSIM 9.0 software. The parameters of various components used in the proposed TLIFB DC-DC converter are given in table II.

A comparator is used to generate the gating pulses. A triangular wave and a DC signal are compared to get the PWM signals for the switches S_1, S_4, S_5, S_8 . The inverted signals of switches S_1, S_4, S_5, S_8 is given to S_3, S_2, S_7, S_6 . The gating pulse waveforms are shown in Fig. 5. A DC voltage of 100V is applied as input. Fig. 6 shows the input voltage waveform. The output of three level is obtained at the multilevel converter with five voltage levels as shown in Fig. 7. Fig. 8 shows the pure sinusoidal AC output voltage which is obtained after the passive filter. Fig. 9 shows the DC output voltage. The input voltage of 100 volts is boosted to 302 volts.

IV. EXPERIMENTAL SETUP

To generate the gating pulses for the switches in the proposed TLIFB DC-DC converter, 8051 microcontroller is used with IR2110 driver IC. The control circuit is shown in Fig. 10. In the power circuit, the eight main switches and diodes are of standard MOSFET of IRFP250. The clamping diodes are STTH3006. The rectifier diodes are STTH3010.

To initialize the 8051 microcontroller and to generate the signals, a program is written using C coding and executed with the help of Keil software. Flash magic software is used to load the program into the microcontroller. The gating pulses are produced with this hardware setup. The waveforms of gating pulses to the switches S_1, S_3 is shown in Fig. 11.

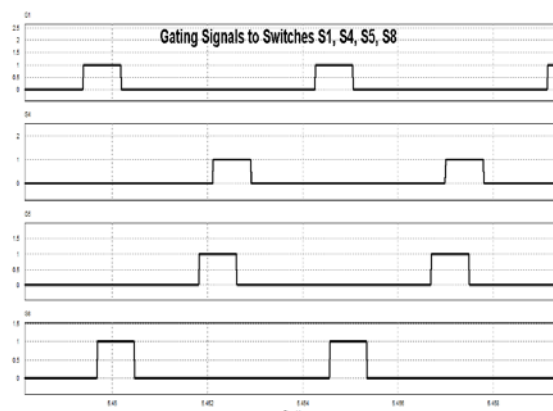


Fig. 5 Waveforms of gating pulses to switches S_1, S_4, S_5, S_8 .

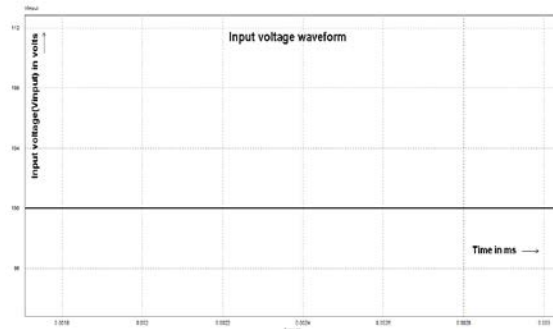


Fig. 6 Input voltage waveform

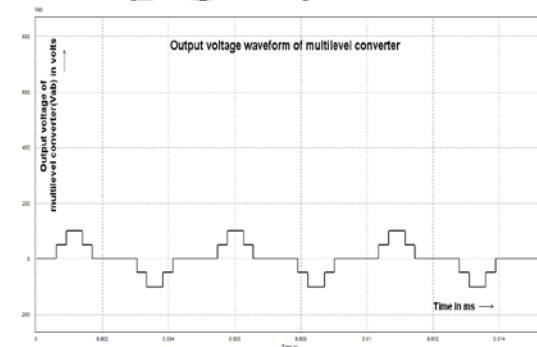


Fig. 7 Output waveform of multilevel converter.

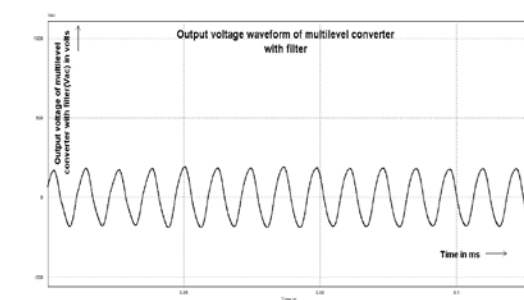


Fig. 8 Output waveform of the multilevel converter with filter.

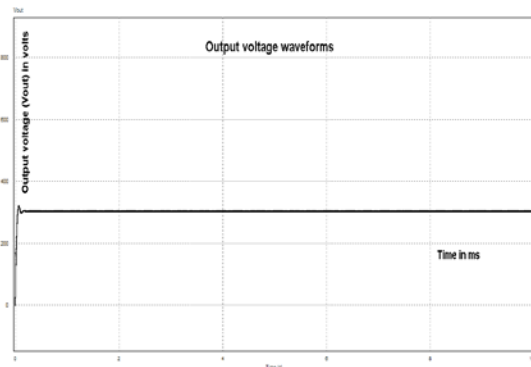


Fig. 9 Output voltage waveform of the proposed TLIFB DC-DC Converter



Fig. 10 Photograph of the designed control circuit of the proposed TLIFB DC-DC Converter

Fig. 12 shows the produced gating signals for the switches S_4 , S_2 . The gating pulses for other switches are produced in the similar manner.

V. CONCLUSION

This paper has presented the TLIFB DC-DC converter for the wind turbine system to facilitate the integration of wind turbines into a dc grid. The proposed two operation modes are discussed in detail where the alternation of the proposed two operation modes can keep the capacitor voltage balanced. The proposed TLIFB DC-DC converter reduces dv/dt rating. It is highly suitable for medium-voltage and high-power conversion. The voltage stress of the power switches is reduced. It can create five-level output voltage to minimize voltage steps. With the usage of passive filter, the voltage stress of the transformer in the TLIFB DC-DC converter can be effectively reduced, which is very significant in the medium-voltage and high-power applications. The

performance of the converter is also improved. Further by

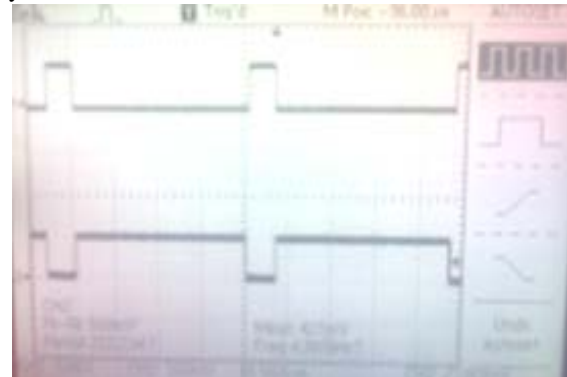


Fig. 11 Waveforms of gating pulses to the switches S_1, S_2

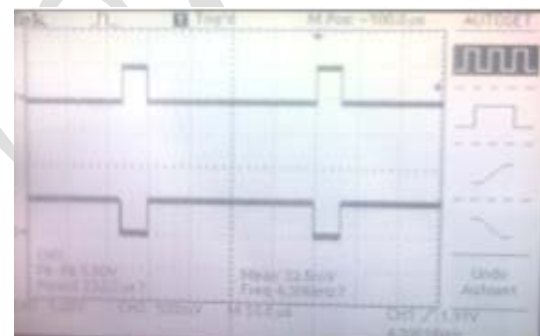


Fig. 12 Waveforms of gating pulses to the switches S_1, S_2

using the TLIFB, the voltage balancing of the converter can be effectively improved. In future, the TLIFB DC/DC converter prototype can be made with high efficiency and good voltage balancing control.

REFERENCES

- [1] B.Wu, Y. Lang, N. Zargari, and S. Kouro, *Power Conversion and Control of Wind Energy Systems*. Hoboken, NJ: Wiley, 2011.
- [2] C. Meyer, M. Hoing, A. Peterson, and R. W. De Doncker, "Control and design of dc grids for offshore wind farms," *IEEE Trans. Ind. Appl.*, vol. 43, no. 6, pp. 1475–1482, Nov./Dec. 2007.
- [3] C.M. Wu, W. H. Lau, and H. Chung, "A five-level neutral-point-clamped H-bridge PWM inverter with superior harmonic suppression: A theoretical analysis," in *Proc. IEEE Int. Symp. Circuits Syst.*, Orlando, FL, May 30–Jun. 2, 1999, vol. 5, pp. 198–201.

- [4] F. Blaabjerg, Z. Chen, and B. S. Kjaer, "Power electronics as efficient interface in dispersed power generation systems," *IEEE Trans. Power Electron.*, vol. 19, no. 5, pp. 1184–1194, Sep. 2004.
- [5] F. Deng and Z. Chen, "Control of Improved Full-Bridge Three-Level DC/DC Converter for Wind Turbines in a DC Grid," *IEEE Trans. Power Electron.*, vol. 28, no. 1, pp. 314–324, Jan. 2013.
- [6] J. Robinson, D. Jovicic, and G. Jo'os, "Analysis and design of an offshore wind farm using a MV DC grid," *IEEE Trans. Power Delivery*, vol. 25, no. 4, pp. 2164–2173, Oct. 2010.
- [7] J. Rodriguez, S. Bernet, B. Wu, J. O. Pontt, and S. Kouro, "Multilevel voltage-source-converter topologies for industrial medium-voltage drives," *IEEE Trans. Ind. Electron.*, vol. 54, no. 6, pp. 2930–2945, Dec. 2007.
- [8] J. R. Pinheiro and I. Barbi, "The three-level ZVS-PWM dc-to-dc converter," *IEEE Trans. Power Electron.*, vol. 8, no. 4, pp. 486–492, Oct. 1993.
- [9] L. Max and S. Lundberg, "System efficiency of a DC/DC converter-based wind farm," *Wind Energy*, vol. 11, no. 1, pp. 109–120, 2008.
- [10] K. Hyosung, K. Jang-Hwan, and S. Seung-Ki, "A design consideration of output filters for dynamic voltage restorers," in *Proc. 35th IEEE Power Electron. Spec. Conf.*, 2004, pp. 4268–4272.
- [11] M. Saeedifard and R. Iravani, "Dynamic performance of a modular multilevel back-to-back HVDC system," *IEEE Trans. Power Delivery*, vol. 25, no. 4, pp. 2903–2912, Oct. 2010.
- [12] N. Mohan, T. M. Undeland, and W. P. Robbins, *Power Electronics: Converters, Applications, and Design*, 3rd ed. New York: Wiley, 2003. K. Hyosung, K. Jang-Hwan, and S. Seung-Ki, "A design consideration of output filters for dynamic voltage restorers," in *Proc. 35th IEEE Power Electron. Spec. Conf.*, 2004, pp. 4268–4272.
- [13] N. Y. Dai, M. C. Wong, and Y. D. Han, "Application of a three-level NPC inverter as a three-phase four-wire power quality compensator by generalized 3DSVM," *IEEE Trans. Power Electron.*, vol. 21, no. 2, pp. 440–449, Mar. 2006.
- [14] P. J. Grbovic, "High-voltage auxiliary power supply using seriesconnected MOSFETs and loating self-driving technique," *IEEE Trans. Ind. Electron.*, vol. 56, no. 5, pp. 1446–1455, May 2009.
- [15] P. J. Grbovi'c, P. Delarue, P. Le Moigne, and P. Bartholomeus, "A bidirectional three-level dc- c converter for the ultracapacitor applications," *IEEE Trans. Ind. Electron.*, vol. 57, no. 10, pp. 3415–3430, Oct. 2010.
- [16] S. Kenzelmann, A. Rufer, M. Vasiladiotis, D. Dujic, F. Canales, and Y. R. de Novaes, "A versatile dc-dc converter for energy collection and distribution using the modular multilevel converter," in *Proc. 14th Eur. Conf. Power Electron. Appl.*, Aug./Sep. 2011, pp. 1–10.
- [17] X. Ruan, B. Li, Q. Chen, S. C. Tan, and C. K. Tse, "Fundamental considerations of three-level dc-dc converters: Topologies, analyses, and control," *IEEE Trans. Circuits Syst. I, Reg. Papers*, vol. 55, no. 11, pp. 3733–3743, Dec. 2008.
- [18] Z. Cheng and B. Wu, "A novel switching sequence design for five-level NPC/H-bridge inverters with improved output voltage spectrum and minimized device switching frequency," *IEEE Trans. Power Electron.*, vol. 22, no. 6, pp. 2138–2145, Nov. 2007.